PHYSICAL REVIEW B **78**, 041406(R) (2008)

Lattice expansion in nonoxidized FePt nanoparticles: X-ray absorption measurements

C. Antoniak, A. Trunova, M. Spasova, M. Farle, and H. Wende
Fachbereich Physik and Center for Nanointegration Duisburg-Essen (CeNIDE), Universität Duisburg-Essen, Lotharstrasse 1, D-47048 Duisburg, Germany

F. Wilhelm and A. Rogalev
European Synchrotron Radiation Facility (ESRF), Boîte Postale 220, F-38043 Grenoble Cedex, France
(Received 27 March 2008; revised manuscript received 10 June 2008; published 22 July 2008)

Wet-chemically synthesized FePt nanoparticles were structurally characterized not only in the as-prepared state but also after the removal of organic ligands and reduction in Fe oxides by a soft *in situ* hydrogen plasma treatment. By the analyses of the extended x-ray absorption fine structures at the Pt L_3 absorption edge, we found an enhanced lattice constant with respect to the bulk material for the oxide-free nanoparticles with clean surfaces. This shows that there exists a lattice expansion in FePt nanoparticles, which is an intrinsic property of the particles, and neither caused by Fe oxides at the surface nor by the organic ligands surrounding the nanoparticles in the as-prepared state. In addition, a first evidence of an inhomogeneous composition within the nanoparticles is given.

DOI: 10.1103/PhysRevB.78.041406 PACS number(s): 61.46.Df, 61.05.cj

The properties of ensembles of self-assembled nanoparticles are currently the subject of intense research activities[1–4] driven both by fundamental interest and their possible use as ultrahigh density storage media.[5,6] Prime candidates for technological applications are nanoparticles of Fe_xPt_{1-x} alloys around the equiatomic stoichiometry in the chemically ordered $L1_0$ state, with its high magnetocrystalline anisotropy of about 6×10^6 J/m^3 in the bulk material.[7,8] In the as-prepared state, wet-chemically synthesized FePt nanoparticles are surrounded by long-chain organic ligands, which drive the self-assembly of nanoparticles when brought onto a substrate and prevent aggregation. The formation of the $L1_0$ phase is driven by volume diffusion and is kinetically suppressed. The disorder-order transformation can be induced by thermal annealing at temperatures between 500 °C and 600 °C for FePt thin films[9,10] and nanoparticles (Ref. 11). In order to understand thermally activated diffusion processes in FePt nanoparticles, it is useful to analyze the crystal structure, especially the influence surface oxides, and the homogeneity of the alloy after the synthesis.

To investigate the local structure, coordination, and composition, the analysis of the extended x-ray-absorption fine structure (EXAFS) is a powerful tool. In this Rapid Communication, we focus on the effect of lattice expansion in FePt nanoparticles (Ref. 12) and investigate whether this expansion is an intrinsic property of the particles or caused by Fe oxides at the surface or the organic ligands surrounding the nanoparticles after synthesis. Therefore, the EXAFS of the nanoparticles was measured in the as-prepared state as well as after a soft hydrogen plasma treatment that removes all the organic ligands and reduces the Fe oxides that may be present at the surface.[13]

Monodisperse single-crystalline FePt particles were prepared by the reduction of $Pt(acac)_2$ and thermal decomposition of $Fe(CO)_5$ as described elsewhere.[7] From transmission electron microscope (TEM) and scanning electron microscope (SEM) images, the size distribution was found to be a log-normal distribution around the mean diameter $d=4.4$ nm with a standard deviation of $\sigma=0.14$. The particles tend to self-assemble hexagonally in dendritic structure as can be seen in Fig. 1(a). The mean center-to-center distance within the covered area is $d_{cc}\approx7$ nm. Energy-dispersive x-ray spectroscopy (EDX) in the TEM shows that the composition averaged over a few nanoparticles is at (56 ± 6) at% Fe content.

As a reference, a bulk sample of a chemically disordered polycrystalline $Fe_{56}Pt_{44}$ alloy was prepared by arc melting under argon atmosphere.

We found by the analysis of the x-ray diffraction (XRD) shown in Fig. 1 that the lattice constant is enhanced by 1%–2% in nanoparticles with a diameter of around 4.4 nm. In larger particles with a diameter of 6.3 nm and an Fe con-

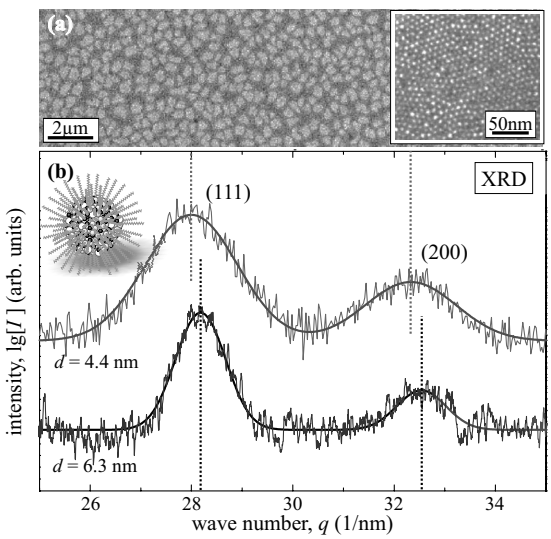

FIG. 1. (a) SEM images at different resolutions of $Fe_{56}Pt_{44}$ nanoparticles with a mean diameter around 4.4 nm on a naturally oxidized Si wafer and (b) XRD of FePt nanoparticles with mean diameters of 4.4 nm (upper diffractogram) or 6.3 nm (lower diffractogram). The particles are in the as-prepared state and surrounded by organic ligands as schematically shown in the inset.

 ©2008 The American Physical Society

TABLE I. Lattice constants determined with different methods for FePt bulk material and nanoparticles (NPs) at room temperature.

FePt system	Lattice constant (nm)
Bulk	0.384 ± 0.002 (XRD)
	0.383 ± 0.003 (EXAFS)
NPs, $d=6.3$ nm, as-prepared	0.384 ± 0.003 (XRD)
NPs, $d=4.4$ nm, as-prepared	0.388 ± 0.002 (XRD)
	0.389 ± 0.006 (ED)
NPs, $d=4.4$ nm, cleaned	0.387 ± 0.004 (EXAFS)

tent of 50 at%, the lattice constant is the same as in the corresponding bulk material $[(0.384 \pm 0.002)$ nm] at room temperature. The difference in the XRD peak positions for nanoparticles with different diameters is significant. In Fig. 1, the logarithm of the XRD intensity is shown as a function of wave number $q=4\pi \sin[\theta]/\lambda$ for FePt nanoparticles with mean diameters of 4.4 and 6.3 nm in the upper and lower diffractogram, respectively. The positions of the (111) and (200) diffraction peaks are marked by vertical dashed lines and are shifted to smaller wave numbers for the smaller particles. This shift is too large to be explained by the slightly different Fe content and indicates a lattice expansion in the smaller FePt nanoparticles, which was confirmed by the high-resolution (HR) TEM images and electron diffraction (ED). The absolute values of the lattice constants are summarized in Table I.

With all these techniques, the lattice constant of the nanoparticles in the as-prepared state is measured, i.e., the lattice constant of nanoparticles containing Fe oxides and surrounded by organic ligands. By the analysis of the EXAFS oscillations of oxide- and ligand-free nanoparticles on the one hand and nanoparticles in the as-prepared state on the other hand, a lattice expansion due to oxides and organic ligands can be distinguished from an intrinsic one as presented in this work.

X-ray absorption measurements were performed at the Pt L_3 absorption edge, and the corresponding EXAFS region at the ID12 beamline of the European Synchrotron Radiation Facility (ESRF) in Grenoble, France, in an energy range of 11.529–12.581 keV in the fluorescence yield (FY) mode. A plasma chamber was attached to the experimental endstation for an *in situ* cleaning of the nanoparticles. In previous studies,[11] we found by the analyses of the x-ray absorption near-edge structure (XANES) at the Fe $L_{3,2}$ absorption edges in the soft x-ray regime that the Fe oxides, which are present in the nanoparticles in the as-prepared state can be reduced by hydrogen plasma for 15 min at a pressure of 5 Pa. In addition, all the organic ligands surrounding the wet-chemically synthesized nanoparticles are removed by the plasma.[14]

To ensure that the Fe oxides of the nanoparticles are reduced, measurements of the XANES at the Fe K edge were performed, which is a sensitive monitor for oxidation as shown in Fig. 2. The XANES of the as-prepared nanoparticles is very similar to the nanocrystalline γ-Fe_2O_3 (Ref. 15). The small differences can be explained by the fact that

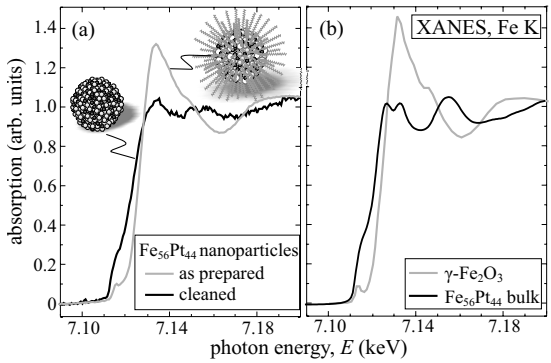

FIG. 2. (a) XANES at room temperature at the Fe K edges of $Fe_{56}Pt_{44}$ nanoparticles in the as-prepared state and after reduction of Fe oxides and (b) reference spectra of metallic Fe in $Fe_{56}Pt_{44}$ bulk material and of nanocrystalline γ-Fe_2O_3 (Ref. 15) are shown for comparison.

the XANES of FePt nanoparticles in the as-prepared state is a superposition of signals from Fe oxides and Fe in a metallic environment. The XANES of the plasma-treated nanoparticles differs significantly from the one in the as-prepared state. Even after more than 24 h in the experimental UHV chamber, the XANES is similar to the reference spectrum of $Fe_{56}Pt_{44}$ bulk material with negligible contributions of Fe oxides.

To extract the measured EXAFS of the nanoparticles at the Pt L_3 absorption edge from the absorption spectrum for further analyses, the background was fitted and subtracted from the experimental data using the AUTOBK algorithm[16] with a threshold of $R_{bkg}=0.11$ nm. For Fourier transformation of the experimental data, the k weighted data were used in the range between $k_{min}=20/\text{nm}$ and $k_{max}=125/\text{nm}$ in a Kaiser-Bessel window with $dk=0.1/\text{nm}$.

The EXAFS function $\chi(k)$ can be expressed by a cumulant expansion with the first cumulant corresponding to the averaged value and the second cumulant corresponding to the mean-square relative displacement. A possible anharmonicity of the interatomic potential is given by the third cumulant c_3, which may be important in the nanoparticles due to a flat and asymmetric potential at the surface caused by a reduced coordination number.

The calculation of the scattering paths and the calculation of $\chi(k)$ was done using the software ARTEMIS based on the algorithms of the FEFFIT (Ref. 17) and FEFF (Refs. 18 and 19) programs.[20] For the calculations, it is necessary to put in the structure of the material, i.e., the Fe and Pt atoms have to be placed at the lattice points of an fcc lattice. Since our samples are chemically disordered, $\chi(k)$ was calculated as the sum of the weighted EXAFS of a Pt absorber atom in a pure Pt environment and in a pure Fe environment with the same lattice constants, i.e., the number of Fe and Pt nearest-neighbor atoms was used as a parameter to fit the simulation to the experimental data. Further fit parameters are an overall energy shift, path-length corrections, and the mean-square relative displacement of the atoms.

It can be clearly seen in Fig. 3 that: (i) the frequency of the oscillations from the bulk reference sample is smaller than those from the nanoparticles and (ii) there is no differ-

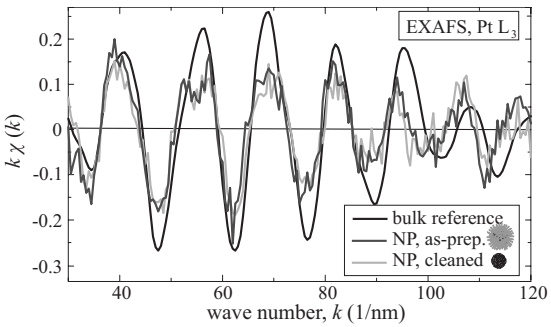

FIG. 3. Room temperature oscillations of the x-ray absorption in the EXAFS regime as a function of the wave number for a bulk $Fe_{56}Pt_{44}$ sample (black line), $Fe_{56}Pt_{44}$ nanoparticles in the as-prepared state (dark gray line) and the same nanoparticles after removal of oxides, and organic ligands (light gray line).

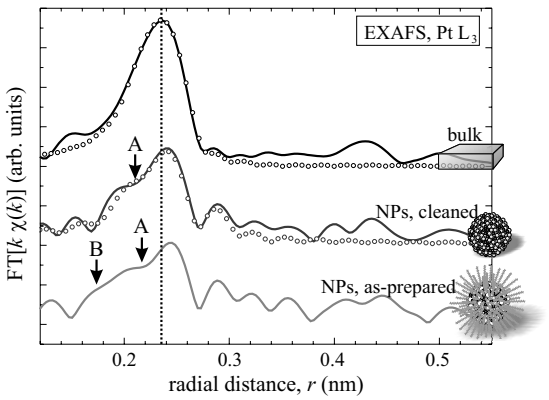

FIG. 4. Magnitude of the Fourier-transformed EXAFS at the Pt L_3 edges for a bulk $Fe_{56}Pt_{44}$ reference sample (black line) and nanoparticles (NPs) of the same averaged composition after plasma cleaning (dark gray line), and in the as-prepared state (light gray line). Lines represent experimental data; circles represent simulated data.

ence in the frequency of the EXAFS oscillations from nanoparticles in the as-prepared state and from plasma-cleaned nanoparticles. The difference between the oscillations from the bulk sample and the oscillations from the nanoparticles cannot be explained by an enhanced c_3, since $c_3 \neq 0$ yields a streching of the EXAFS at higher k values, which is not observed here. Even with a small but reasonable value of $c_3 = 10^{-7}$ nm^3 it is not possible to simulate the experimental data properly. Therefore, it can be concluded that: (i) the lattice expansion within the $Fe_{56}Pt_{44}$ nanoparticles with respect to the corresponding bulk material is confirmed and (ii) the lattice expansion is not caused by Fe oxides or the organic ligands surrounding the particles, but it is an intrinsic property of the nanoparticles.

In the Fourier transform of the EXAFS signal (Fig. 4), the different lattice constants are indicated by the shift of the main peak position that is connected to the distance between nearest-neighbor atoms. Note that there is a shift between the peak position of the Fourier transform and the geometrical distance between nearest-neighbor atoms at about 0.03–0.04 nm because of the EXAFS phase shift.

In the as-prepared state, the Fourier-transformed EXAFS exhibits a broadening of the main peak with a shoulder around $r = 0.16$ nm, typical for oxygen (denoted as "*B*" in Fig. 4). A minimum in the amplitude at about 0.21 nm (denoted as "*A*" in Fig. 4) for both the nanoparticles in the as-prepared state and after plasma cleaning indicates a sharp minimum in backscattering amplitude at $k \approx 60/\text{nm}$ that is known in literature as Ramsauer-Townsend effect.[21] The reduction in the scattering amplitude over a small region in k space exists for several elements with atomic numbers near 80, such as Pt ($Z = 78$) (Ref. 22), but for most elements (e.g., Fe) the scattering amplitude varies slowly as a function of k. Therefore, the clear enhancement of this feature in the EXAFS of the FePt nanoparticles with respect to the EXAFS in the FePt bulk material gives evidence for Pt enrichment around the Pt absorber atoms, i.e., an inhomogeneous composition within the nanoparticles. This local deviation of the averaged composition may explain, e.g., the reduced magnetic moments at the Fe sites experimentally obtained in FePt nanoparticles (Refs. 11 and 23). A more detailed EXAFS analysis and discussion of the influence on the magnetic properties will be given elsewhere.

The lattice constants extracted from the EXAFS data by simulation of the experimental data given in Table I are in good agreement to the lattice constants determined by XRD or ED, confirming the lattice expansion in small FePt nanoparticles.

In conclusion, we found a lattice constant in FePt nanoparticles with a mean diameter of about 4.4 nm that is enhanced by 1%–2% with respect to the lattice constant of the corresponding bulk material. For larger particles with a mean diameter of about 6.3 nm, the same lattice constant was obtained as in the bulk material within experimental error bars. The lattice expansion in small FePt nanoparticles is an intrinsic property of the nanoparticles and is not caused by surface oxidation. In addition, the Fourier-transformed EXAFS gives evidence for an inhomogeneous composition within the nanoparticles.

We would like to thank S. Sun (Brown U.) for the synthesis of the nanoparticles, T. Krenke and M. Acet (U. Duisburg-Essen) for providing the bulk reference sample, and K. Fauth (U. Würzburg) for helpful comments on this manuscript and useful discussions. For help in the preparation of the experiment, P. Voisin and S. Feite (ESRF) are gratefully acknowledged. This work was supported by the DFG (SFB445), the ESRF, and the EU (MRTN-CT-2004-0055667, "SyntOrbMag").

[1] R. W. Chantrell, D. Weller, T. J. Klemmer, S. Sun, and E. E. Fullerton, J. Appl. Phys. **91**, 6866 (2002).
[2] M. Spasova, U. Wiedwald, R. Ramchal, M. Farle, and M. Hilgendorff, J. Magn. Magn. Mater. **240**, 40 (2002).
[3] V. F. Puntes, K. M. Krishnan, and P. Alivisatos, Appl. Phys. Lett. **78**, 2187 (2001).
[4] C. Antoniak, J. Lindner, and M. Farle, Europhys. Lett. **70**, 250 (2005).
[5] S. Sun and C. B. Murray, J. Appl. Phys. **85**, 4325 (1999).
[6] J. L. Dorman, D. Fiorani, and E. Tronc, Adv. Chem. Phys. **98**, 283 (1997).
[7] S. Sun, C. B. Murray, D. Weller, L. Folks, and A. Moser, Science **287**, 1989 (2000).
[8] T. Shima, K. Takanashi, Y. K. Takahashi, and K. Hono, Appl. Phys. Lett. **85**, 2571 (2004).
[9] M. R. Visokay and R. Sinclair, Appl. Phys. Lett. **66**, 1692 (1995).
[10] J.-U. Thiele, L. Folks, M. F. Toney, and D. Weller, J. Appl. Phys. **84**, 5686 (1998).
[11] C. Antoniak, J. Lindner, M. Spasova, D. Sudfeld, M. Acet, M. Farle, K. Fauth, U. Wiedwald, H.-G. Boyen, P. Ziemann, F. Wilhelm, A. Rogalev, and S. Sun, Phys. Rev. Lett. **97**, 117201 (2006).
[12] R. M. Wang, O. Dmitrieva, M. Farle, G. Dumpich, H. Q. Ye, H. Poppa, R. Kilaas, and C. Kisielowski, Phys. Rev. Lett. **100**, 017205 (2008).
[13] H.-G. Boyen, K. Fauth, B. Stahl, P. Ziemann, G. Kästle, F. Weigl, F. Banhart, M. Heßler, G. Schütz, N. S. Gajbhije, J. Ellrich, H. Hahn, M. Büttner, M. G. Garnier, and P. Oelhafen, Adv. Mater. (Weinheim, Ger.) **17**, 574 (2005).
[14] C. Antoniak and M. Farle, Mod. Phys. Lett. B **21**, 1111 (2007).
[15] E. Pellegrin, M. Hagelstein, S. Doyle, H. O. Moser, J. Fuchs, D. Vollath, S. Schuppler, M. A. James, S. S. Saxena, L. Niesen, O. Rogojanu, G. A. Sawatzky, C. Ferrero, M. Borowski, O. Tjernberg, and N. B. Brookes, Phys. Status Solidi B **215**, 797 (1999).
[16] M. Newville, P. Livińš, Y. Yacoby, J. J. Rehr, and E. A. Stern, Phys. Rev. B **47**, 14126 (1993).
[17] M. Newville, J. Synchrotron Radiat. **8**, 322 (2001).
[18] A. L. Ankudinov, B. Ravel, J. J. Rehr, and S. D. Conradson, Phys. Rev. B **58**, 7565 (1998).
[19] S. I. Zabinsky, J. J. Rehr, A. Ankudinov, R. C. Albers, and M. J. Eller, Phys. Rev. B **52**, 2995 (1995).
[20] B. Ravel and M. Newville, J. Synchrotron Radiat. **12**, 537 (2005).
[21] H. Faxén and J. Holtsmark, Z. Phys. **45**, 307 (1927).
[22] A. G. McKale, B. W. Veal, A. P. Paulikas, S.-K. Chan, and G. S. Knapp, Phys. Rev. B **38**, 10919 (1988).
[23] O. Dmitrieva, M. Spasova, C. Antoniak, M. Acet, G. Dumpich, J. Kästner, M. Farle, K. Fauth, U. Wiedwald, H.-G. Boyen, and P. Ziemann, Phys. Rev. B **76**, 064414 (2007).